

Reduced-Order Modelling of Nonlinear Aircraft Structures

Guanqun Gai

guanqun.gai@liverpool.ac.uk

PhD Student
School of Engineering
University of Liverpool
United Kingdom

Sebastian Timme

sebastian.timme@liverpool.ac.uk

Lecturer
School of Engineering
University of Liverpool
United Kingdom

Kenneth J. Badcock

k.j.badcock@liverpool.ac.uk

Pro Vice Chancellor, Professor
School of Engineering
University of Liverpool
United Kingdom

ABSTRACT

An application of nonlinear model reduction for a full-scale passenger aircraft, exhibiting geometric structural nonlinearity, is presented. The model reduction approach is based on eigenmode decomposition about the coupled aeroelastic system's reference equilibrium point combined with a projection of the expanded full-order nonlinear residual function. Efforts are made to establish a structured approach to identify the dominant modes required to construct an accurate reduced-order model for such nonlinear aeroelastic system. Time-domain results for gust response analysis are then presented to study the effect of structural nonlinearities and to compare the reduced model against the full-order simulation. Results show both the linear and nonlinear reduced-order models are capable of accurately predicting the dynamic gust response of aircraft structures while achieving significant reduction in system size.

1.0 Introduction

This paper presents an application of nonlinear model reduction for the dynamic gust response analysis of realistic full-scale aircraft configurations exhibiting geometric structural nonlinearities. This investigation builds upon previous work[1] which extended the model reduction framework to include higher order nonlinearity and demonstrated accurate prediction of aeroelastic responses of a nonlinear two degree-of-freedom aerofoil model. The model reduction approach further builds upon the work in [2, 3] and is based on eigenmode decomposition about the coupled aeroelastic system's reference equilibrium point combined with a projection of the expanded full-order nonlinear residual function. Current model reduction application deals with multiple eigenmodes[2, 4, 5] and the linear formulation has been applied to realistic aircraft configurations where the aerodynamics are modelled by a commercial computational fluid dynamics code[3].

An large body of work focusing on the geometrically exact structural nonlinearity of very flexible aircraft structures. A complete aeroelastic formulation for a HALE type aircraft is presented in [6], while a strain-based finite element beam framework to model such an aircraft is studied in [7]. The nonlinear aeroelastic modelling for a fully flexible aircraft is studied in [8]. Later, the effect of discrete gust disturbances on a flying wing model is studied in [9]. More recently, several investigations have been presented combining geometric structural nonlinearity, flight dynamics and unsteady aerodynamics for flying wings [10, 11] and a framework to study the behaviour of slender wings in incompressible flow is described in [12].

This paper examines the effect of a geometrically exact nonlinear beam formulation as applied to the FFAST aircraft model. The physical structural model is detailed in Section 2 with the geometrically exact beam equations [13, 14] described in Subsection 2.1 and aerodynamics based on the linear theories of Wagner and Küssner briefly outlined in Subsection 2.2. This paper aims to demonstrate the application of model reduction on a full-scale aircraft structure. The model reduction is formulated in Section 3. A guideline to determine the important modes used for model reduction is discussed in Section 4. Results are presented in Section 5.

2.0 Physical Model

The FFAST aircraft (Fig. 1) is constructed by hand using the nonlinear beam model as discussed hereafter in Subsection 2.1. The beam-stick model consists of 11 elements along the fuselage centre-line, 11 elements for each main wing, and 8 elements per lifting surface at the tail. Both the fuselage and wings vary in geometric properties along their respective lengths. The material density is 2000 kgm^{-3} , with a Poisson ratio of 0.3. The default stiffness for the fuselage beams is $1.5 \times 10^{11} \text{ Pa}$, while for the wing elements it is $1.8 \times 10^{11} \text{ Pa}$. The entire structure consists of 59 unconstrained nodes and has a total of 1180 degrees-of-freedom when coupled with strip aerodynamics as discussed in Subsection 2.2.

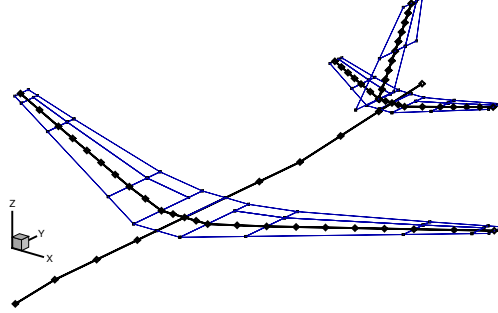


Figure 1. Finite element beam-stick model of FFAST aircraft

The FFAST wing model is obtained by taking one of the wings from the FFAST aircraft model and clamping the wing at the root. The wing features sweep, dihedral and inhomogeneous geometric properties along the spanwise direction. The FFAST wing consists of 11 unconstrained structural nodes leading to a total of 220 degrees-of-freedom when coupled strip aerodynamics.

2.1 Geometrically Exact Beam Model

The nonlinear beam model [13, 14] in general couples structural flexibility with unrestrained rigid-body motions. The descriptions of beam kinematics is geometrically exact. The finite element discretised form of the equations of motion for a discrete restrained beam is given as follows

$$M(\mathbf{X}_e) \ddot{\mathbf{X}}_e + \mathbf{Q}_{\text{gyr}}(\mathbf{X}_e, \dot{\mathbf{X}}_e) + \mathbf{Q}_{\text{stiff}}(\mathbf{X}_e) = \mathbf{Q}_{\text{ext}}(\mathbf{X}_e, \dot{\mathbf{X}}_e) \quad (1)$$

Here, \mathbf{X}_e denotes the vector of nodal displacements and rotations, while $M(\mathbf{X}_e)$ is the tangent mass matrix. The vectors \mathbf{Q}_{gyr} , $\mathbf{Q}_{\text{stiff}}$ and \mathbf{Q}_{ext} represent the gyroscopic, elastic and external forces, respectively. The expression for the external forces is general and typically a function of the system states. This is characteristic of, for example, aerodynamic or other externally applied follower forces both of which are dependent on the structure's geometry.

Equation (1) is linearised around the equilibrium giving the incremental form of the finite element equation of motion as

$$M(\mathbf{x}_e) \ddot{\mathbf{x}}_e + C(\mathbf{x}_e, \dot{\mathbf{x}}_e) \dot{\mathbf{x}}_e + K(\mathbf{x}_e) \mathbf{x}_e = \Delta \mathbf{Q}_{\text{ext}}(\mathbf{x}_e, \dot{\mathbf{x}}_e) \quad (2)$$

with \mathbf{x}_e denoting a disturbance from the equilibrium position. This final second-order differential equation can be rearranged into first-order form for the application of model reduction.

2.2 Aerodynamic Model

Linear aerodynamic strip theory is coupled with the beam equations by assuming each structural node coincides with a two-dimensional aerofoil section and therefore the aerodynamic forces acting on each aerofoil directly translate to the structural nodes. The aerodynamic model uses Wagner and Küssner functions to describe the aerodynamic forces due to aerofoil motion and gust disturbances, respectively. This aerodynamic model is used in previous work and has been verified against common results in literature[1].

The aerodynamic strip system is defined with respect to the ‘beam’ reference frame located at the wing root with the x -axis pointing along the span of the wing, the y -axis along the streamwise direction and the z -axis perpendicular up. Each structural node j in the nonlinear finite element beam model coincides with a two-dimensional aerofoil section in the y - z plane. The aerodynamic forces acting on each aerofoil section will depend on the sectional motion and are in addition, treated as follower forces.

3.0 Nonlinear Model Reduction

The coupled nonlinear model describing the dynamics of an elastic aircraft system can be represented in semi-discrete state-space form. Denote by \mathbf{W} the n -dimensional state-space vector partitioned into structural states \mathbf{W}_s and aerodynamic states \mathbf{W}_f . Written as a set of first-order ordinary differential equations, we find

$$\dot{\mathbf{W}} = \mathbf{R}(\mathbf{W}, \boldsymbol{\Theta}) \quad (3)$$

where \mathbf{R} is the nonlinear residual vector corresponding to the unknowns \mathbf{W} , while $\boldsymbol{\Theta}$ is a vector of independent system parameters. There exists a reference equilibrium point \mathbf{W}_0 for given constants $\boldsymbol{\Theta}_0$.

Define an increment with respect to the equilibrium as $\mathbf{w} = \mathbf{W} - \mathbf{W}_0$. The nonlinear residual in Eq. (3) can then be expanded in a multi-variate Taylor series about the reference equilibrium point with respect to the system states \mathbf{W} as

$$\mathbf{R}(\mathbf{W}, \boldsymbol{\Theta}) \approx A\mathbf{w} + \frac{1}{2!}\boldsymbol{\mathcal{B}}(\mathbf{w}, \mathbf{w}) + \left(\mathbf{R}_{\boldsymbol{\Theta}}(\mathbf{W}_0, \boldsymbol{\Theta}_0) + A_{\boldsymbol{\Theta}}\mathbf{w} + \frac{1}{2!}\boldsymbol{\mathcal{B}}_{\boldsymbol{\Theta}}(\mathbf{w}, \mathbf{w}) \right) \boldsymbol{\theta} \quad (4)$$

where $A = \partial\mathbf{R}/\partial\mathbf{W}$ is the system Jacobian matrix and $\boldsymbol{\mathcal{B}}$, the symmetric multilinear vector function of second-order derivatives, is retained. More specifically, evaluated about the equilibrium point (indicated by subscript 0), it is expressed as

$$\boldsymbol{\mathcal{B}}(\mathbf{x}, \mathbf{y}) = \sum_{j,k=1}^n \left. \frac{\partial^2 \mathbf{R}}{\partial W_j \partial W_k} \right|_0 x_j y_k$$

Subscript $\boldsymbol{\Theta}$ denotes differentiation with respect to it. While only first-order derivatives in $\boldsymbol{\Theta}$ are retained here for this study, in general, higher-order derivatives can be included as well. Equation (4) represents the starting point for the model reduction.

The full-order system is projected onto a small basis of m eigenvectors of the Jacobian matrix A evaluated at the equilibrium point. The eigensolutions of the Jacobian matrix are, in general, complex-valued. Such eigensolutions exist, for example, as modes of structural vibration. For the specific case of the linear aerodynamic model discussed in Subsection 2.2, eigensolutions associated with the fluid unknowns are purely real-valued.

The set of right (direct) eigenvectors ϕ_i is obtained by solving

$$A\phi_i = \lambda_i\phi_i, \quad \text{for } i = 1, \dots, m \quad (5)$$

while the corresponding problem

$$A^H\psi_i = \bar{\lambda}_i\psi_i, \quad \text{for } i = 1, \dots, m \quad (6)$$

gives the set of left (adjoint) eigenvectors ψ_i . The superscript H denotes the conjugate transpose (i.e. Hermitian). The right and left eigenvectors are collected together respectively giving the corresponding modal matrices, denoted by Φ and Ψ ,

$$\Phi = [\phi_1, \dots, \phi_m], \quad \Psi = [\psi_1, \dots, \psi_m], \quad \Phi, \Psi \in \mathbb{C}^{n \times m} \quad (7)$$

It is convenient to scale the eigenvectors to satisfy the biorthonormality conditions,

$$\Psi^H\Phi = I, \quad \Psi^H\bar{\Phi} = O, \quad I, O \in \mathbb{R}^{m \times m} \quad (8)$$

where matrices I and O are the identity matrix and a zero matrix, respectively. The biorthonormality conditions also ensure the following results

$$\Psi^HA\Phi = \Lambda, \quad \Psi^HA\bar{\Phi} = O \quad (9)$$

where $\Lambda \in \mathbb{C}^{m \times m}$ is a diagonal matrix containing the eigenvalues.*

The full-order unknowns \mathbf{w} are described by a small set of m eigenvectors using the following coordinate transformation

$$\mathbf{w} = \Phi\mathbf{z} + \bar{\Phi}\bar{\mathbf{z}} \quad (10)$$

where $\mathbf{z} \in \mathbb{C}^m$ is the state-space vector governing the dynamics of the reduced-order nonlinear system. The unknowns \mathbf{w} are represented as a linear combination of right eigenvectors with \mathbf{z} as the time-dependent amplitude. The nonlinear reduced-order model is then formed by substitution and premultiplying each term by the Hermitian of the left modal matrix. The final nonlinear reduced-order model takes the form

$$\begin{aligned} \dot{\mathbf{z}} = & \Lambda\mathbf{z} + \frac{1}{2!}\Psi^H\mathcal{B}(\Phi\mathbf{z} + \bar{\Phi}\bar{\mathbf{z}}, \Phi\mathbf{z} + \bar{\Phi}\bar{\mathbf{z}}) \\ & + \Psi^H\left(\mathbf{R}_\theta + A_\theta\Phi\mathbf{z} + A_\theta\bar{\Phi}\bar{\mathbf{z}} + \frac{1}{2!}\mathcal{B}_\theta(\Phi\mathbf{z} + \bar{\Phi}\bar{\mathbf{z}}, \Phi\mathbf{z} + \bar{\Phi}\bar{\mathbf{z}})\right)\theta \end{aligned} \quad (11)$$

This is a reduced complex system of equations which can be readily integrated in time.

* Note in the case of a real-valued eigensolution, the biorthonormality conditions can no longer be satisfied as $\phi = \bar{\phi}$. These eigenvectors are then scaled such that $\psi^H\phi = \frac{1}{2}$ giving $\psi^HA\phi = \frac{1}{2}\lambda$ which is convenient in order to use consistent notation when dealing both with real- and complex-valued modes.

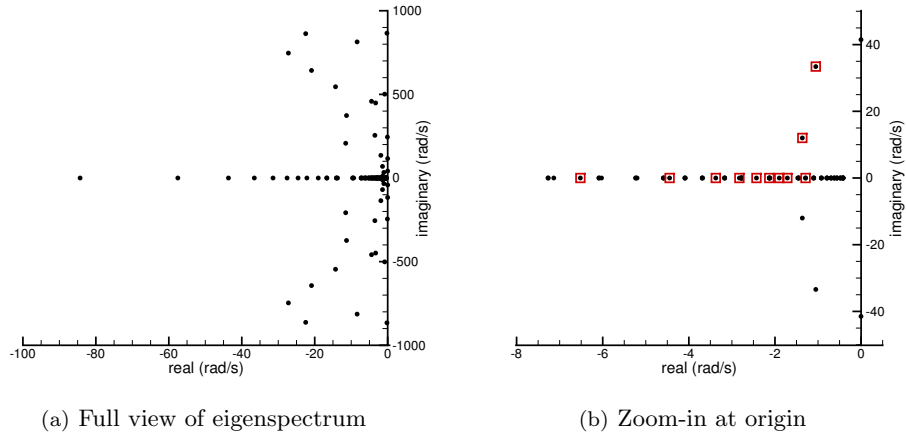


Figure 2. Eigenvalue spectrum of FFAST wing

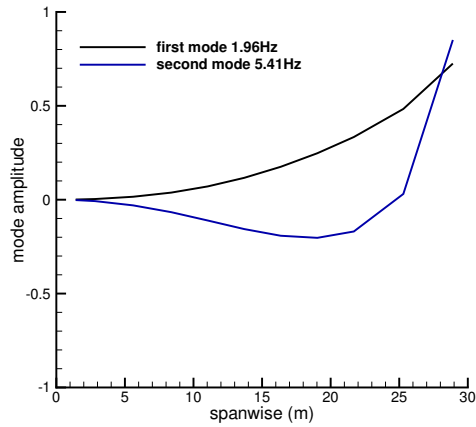


Figure 3. First two bending modes for the isolated wing

4.0 Eigenmode Selection for Model Reduction

The test cases discussed herein, i.e. the FFAST aircraft and corresponding isolated wing, are large structural models where each structural node corresponds to a two-dimensional aerofoil modelled by linear aerodynamic strip theory. To form the reduced-order model for such a system, it is important to identify the basis relevant to the system dynamics. The eigensolution of such a system consists of a large number of purely real-valued eigenvalues arising from the aerodynamic and gust degrees-of-freedom (the fluid unknowns) and complex-conjugate pairs of eigenvalues arising from the structural degrees-of-freedom (the structural unknowns). This is illustrated for the FFAST wing in Fig. 2.

In order to form an accurate reduced-order model it is crucial to retain the first few lower-frequency, weakly damped structural modes which are associated with dominant amplitudes. These take the form of complex-conjugate pairs in the eigensolution. The number of modes depends on the type of structure. In the case of the isolated FFAST wing, the first two lower-frequency structural bending modes (Fig. 3) are found to be sufficient and any additional structural mode give negligible improvement to the reduced-order solution. In the case of the full FFAST aircraft, two additional structural modes associated with the fuselage are needed.

In addition, there exists a series of purely real-valued ‘gust eigenmodes’ which contributes to the accuracy of the structural response during the gust disturbance phase and should be included. These gust eigenmodes can be determined analytically by the expression $\lambda = -\epsilon_3 U/b$, where U is the freestream velocity, b is the local semi-chord length corresponding to the aerofoil sections and $\epsilon_3 = 0.1393$ is the lower time constant used in the exponent in the Küssner function [15]. The accuracy of the solution will improve with increasing number of gust modes starting with the one of the lowest value. The number of gust modes required to achieve a good prediction varies with the total number of aerodynamic strips of the model and it is a good general rule to choose a large number gust modes. From a practical conservative point of view, it is feasible to calculate and include this lower-valued gust mode arising from more than half of all the wing nodes as this is still a minimal fraction of the total system size as will be illustrated in Section 5. For clarity, in Fig. 2 (b) some of these important eigenmodes are highlighted in red.

Similar to gust eigenmodes there exist, corresponding to the time constants of the Wagner function, purely real-valued ‘aerodynamic eigenmodes’ which make up the dominant portion of all eigenvalues on the real axis. The inclusion of these modes were found to have minimal impact on the reduced-order solution for the gust response simulations examined.

5.0 Results

5.1 FFAST Wing

The FFAST wing is simulated for gust response calculation with the aim to analyse the effect of geometric structural nonlinearity and the reduced-order model. The FFAST wing is placed in a freestream flow of 50 ms^{-1} at sea-level and subjected to discrete 1-cos gust disturbance acting in the vertical direction with intensity of 14% of the freestream speed. The amplitude of this gust intensity is chosen high to induce the nonlinear effects. A range of standard gust lengths are evaluated ranging from 9 m to 107 m. Figure 4 (a) shows the response histories of the wing tip to the range of gust lengths with the short length gusts producing highly oscillatory responses while the longer gusts give a smooth damped dynamic response. Since the largest amplitudes are found for gust lengths of 21 m and 107 m, these will be discussed in more detail below. Figure 4 (b) shows the geometrically nonlinear solution at two specific gust lengths of

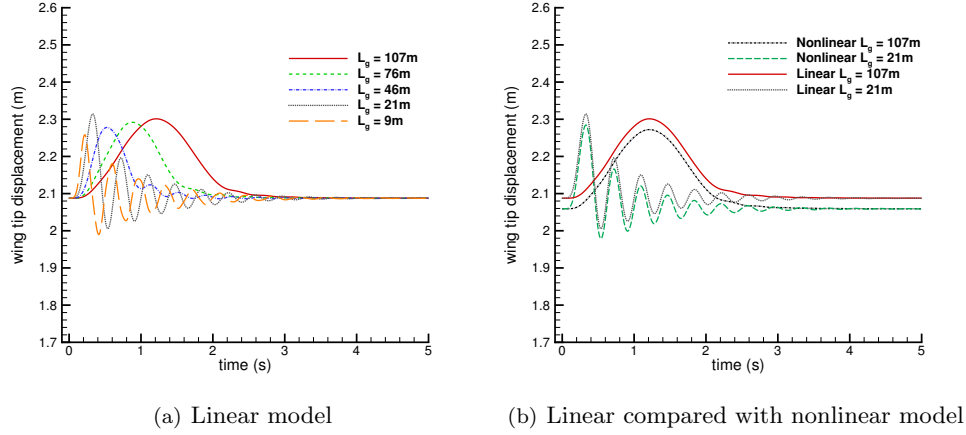


Figure 4. Linear and nonlinear wing tip response to gusts at 50 m/s freestream speed.

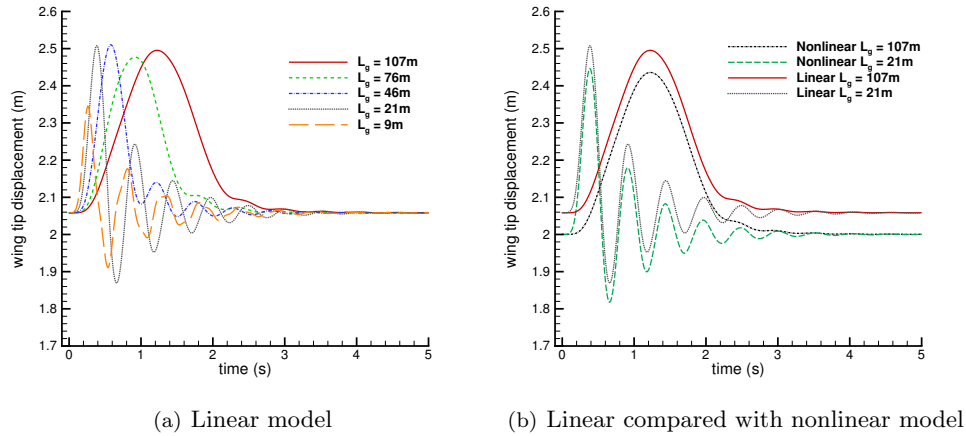


Figure 5. Reduced stiffness linear and nonlinear wing tip response to gusts at 50 m/s freestream speed.

21 m and 107 m. In general, the geometrically nonlinear solution differs moderately from the linear solution and has overall reduced amplitudes in the dynamic response. However, the effect of the geometric nonlinearity is minimal, this is due to the high structural stiffness of the FFAST wing with $E = 1.8 \times 10^{11}$ Pa. For the purpose of emphasising the geometric nonlinear effects all the subsequent results have a reduced material stiffness of $E = 9.0 \times 10^{10}$ Pa. Figure 5 shows equivalent results, compared with Fig. 4, at this reduced structural stiffness. Here, the differences induced by the geometric nonlinear effect is more pronounced.

Next, the application of the linear reduced-order model is considered. This is the case where the term \mathcal{B} is neglected in Eq. (11). Several reduced-order models are constructed based on various numbers of basis eigenmodes. The selection of such

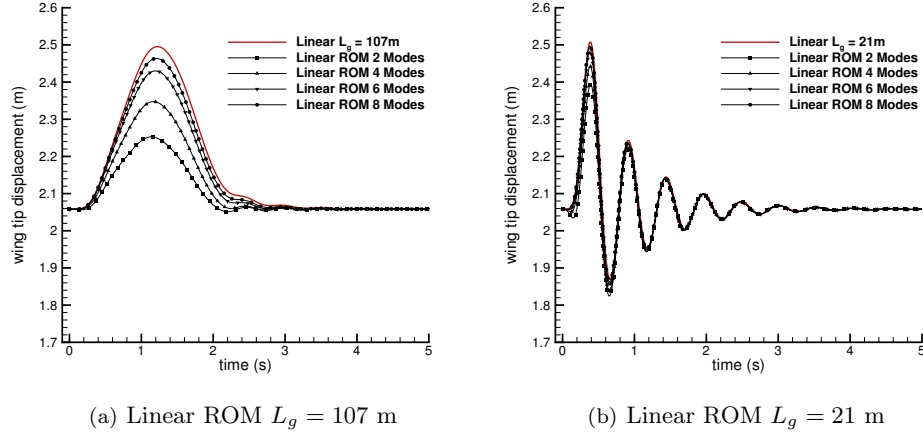


Figure 6. FFAST wing linear reduced-order model at two distinct gust lengths

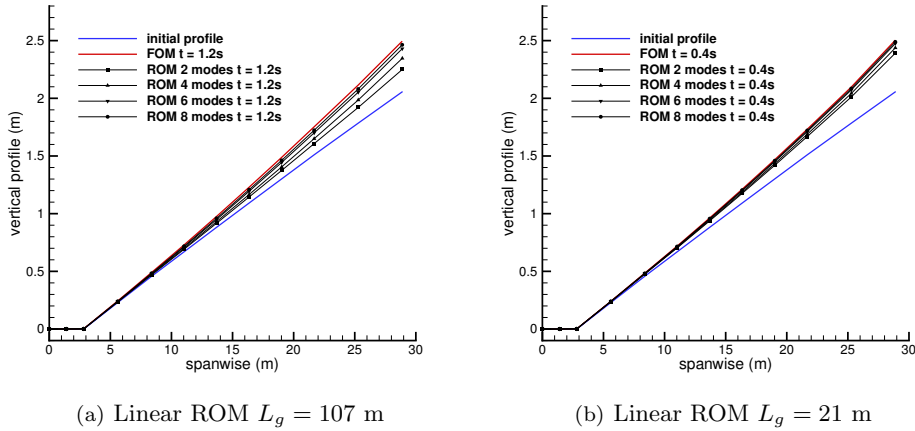


Figure 7. Linear wing profile at maximum amplitude for two distinct gust lengths

eigenmodes follows the method described in Section 4. First, the two lowest-frequency structural modes are used. Then, additional gust modes are included in the reduced-order model basis. The system is simulated under the same two critical gust lengths as previously. Figure 6 shows the results produced by the linear reduced-order models for the wing tip motion history. It is clear that by including additional gust modes the reduced-order model produces incrementally better representations of the full-order solution. The spanwise displacement profile at the maximum amplitude point as produced by the full-order simulation as well as the reduced-order models is shown in Fig. 7. For the long length gust at $L_g = 107$ m this occurs at 1.2 s, and for the short length gust at 0.4 s. It can be observed that by including additional gust modes the solution is improved for all structural nodes. A satisfactory reduced-order model

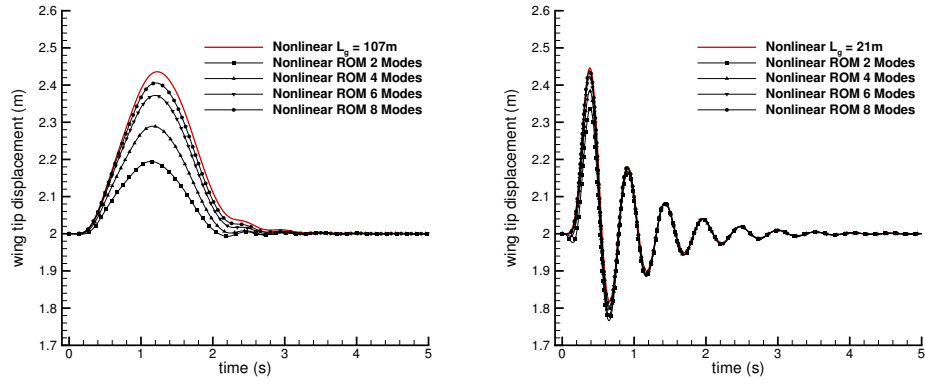
(a) Nonlinear ROM $L_g = 107$ m(b) Nonlinear ROM $L_g = 21$ m

Figure 8. FFAST wing nonlinear reduced-order model at two distinct gust lengths

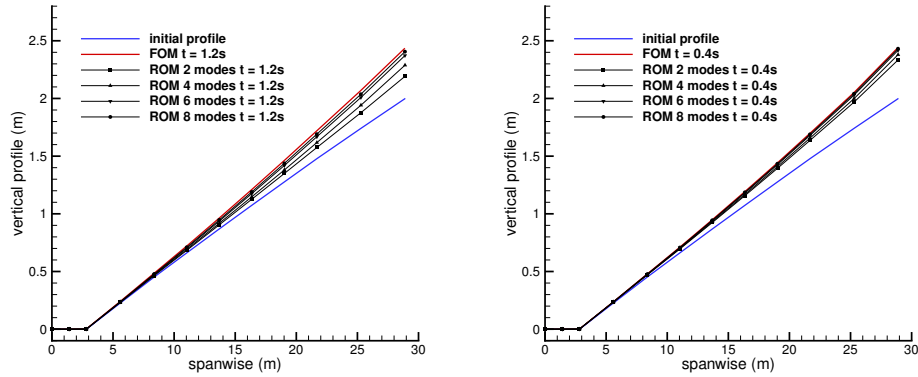
(a) Nonlinear ROM $L_g = 107$ m(b) Nonlinear ROM $L_g = 21$ m

Figure 9. Nonlinear wing profile at maximum amplitude for two distinct gust lengths

solution is obtained using eight modes reducing a full-order system of 220 degrees-of-freedom.

The application of the nonlinear reduced-order model includes the symmetric multilinear vector function of second-order derivatives, \mathcal{B} , in Eq. (11). Figures 8 and 9 show the same set of results for those simulations. The results follow a similar trend compared with the linear case, with the additional feature that the nonlinear reduced-order model is able to capture the lower amplitude of the nonlinear response.

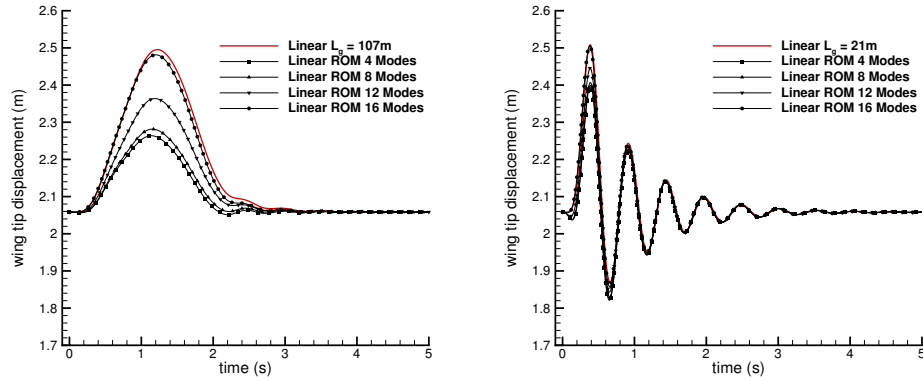
(a) Linear ROM $L_g = 107$ m(b) Linear ROM $L_g = 21$ m

Figure 10. FFAST aircraft linear reduced-order model at two distinct gust lengths

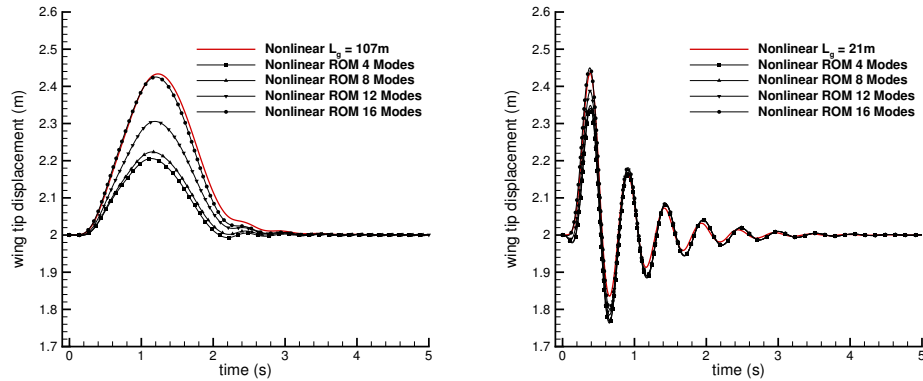
(a) Nonlinear ROM $L_g = 107$ m(b) Nonlinear ROM $L_g = 21$ m

Figure 11. FFAST aircraft nonlinear reduced-order model at two distinct gust lengths

5.2 FFAST Aircraft

The same set of simulations are performed for the full scale FFAST aircraft with reduced stiffness for the wings ($E = 9.0 \times 10^{10}$ Pa) and unaltered stiffness for the fuselage section ($E = 1.5 \times 10^{11}$ Pa). For the linear reduced-order model construction additional basis eigenmodes are required to achieve an accurate prediction of the full-order solution. Initially the first four structural eigenmodes are included. Additional gust modes are added to obtain improving representations of the full order solution. A satisfactory result is achieved with 16 basis eigenmodes in total. This is a reduction of a 1180 degrees-of-freedom system. Figure 10 shows the performance of the linear reduced-order model at the same two gust lengths: $L_g = 107$ m and $L_g = 21$ m. Similar results are obtained by the nonlinear reduced-order model presented in Fig. 11

6.0 Conclusions

This paper presents an application of nonlinear reduced-order modelling applied to full-scale nonlinear aircraft structures for gust response calculations. The test cases herein are based on the FFAST aircraft model which is constructed by hand using a geometrically exact nonlinear beam formulation while the aerodynamics rely on linear strip theory with motion- and gust-induced contributions enforced at each structural node representing a part of the wing. The nonlinear model reduction approach is based on the eigenmode decomposition of the system's Jacobian matrix and projection of the full-order dynamics onto this finite vector space. An approach to identify the important eigenmodes, used as basis in the model reduction, is discussed. Besides the lowest-frequency structural modes, also gust modes should be included if the initial transient response during the gust is to be accurately represented. These gust eigenmodes can always be identified as their corresponding eigenvalues can be calculated by hand.

In general, both the linear and nonlinear (up to second order) reduced models show accurate prediction with respect to their corresponding linear and geometrically nonlinear full order solutions when simulating gust encounter at a range of gust lengths. It is important to note that the peak deflection for the structural response is accurately reproduced in the reduced models. For the largest test case, the full aircraft, a reduction in system size from 1180 to 16 is achieved.

Future work will be directed at formulating and establishing higher-order nonlinear reduced-order model terms. The purpose of such development is to investigate the reduced-order model capability when dealing with higher-order structural nonlinearity.

Acknowledgements

The work was supported by an Engineering and Physical Sciences Research Council (EPSRC) Industrial CASE Studentship award and sponsored by Airbus in the UK.

REFERENCES

1. Gai, G. and Timme, S., "Nonlinear reduced-order modelling for limit-cycle oscillation analysis," *Nonlinear Dynamics*, Vol. 84, No. 2, 2015, pp. 991–1009.
2. Da Ronch, A., Badcock, K. J., Wang, Y., Wynn, A., and Palacios, R. N., "Nonlinear model reduction for flexible aircraft control design," *AIAA Paper 2012-4404*, 2012.
3. Timme, S., Badcock, K. J., and Da Ronch, A., "Linear Reduced Order Modelling for Gust Response Analysis using the DLR-TAU Code," *International Forum for Aeroelasticity and Structural Dynamics*, 2013.
4. Da Ronch, A., Tantaroudas, N. D., and Badcock, K. J., "Reduction of Nonlinear Models for Control Applications," *AIAA Paper 2013-1491*, 2013.

5. Da Ronch, A., Tantaroudas, N. D., Timme, S., and Badcock, K. J., "Model Reduction for Linear and Nonlinear Gust Loads Analysis," *AIAA Paper 2013-1492*, 2013.
6. Patil, M. J., Hodges, D. H., and Cesnik, C. E. S., "Nonlinear Aeroelastic Analysis of Complete Aircraft in Subsonic Flow," *Journal of Aircraft*, Vol. 37, No. 5, 2000, pp. 753–760.
7. Cesnik, C. E. S. and Brown, E. L., "Modeling of High Aspect Ratio Active Flexible Wings for Roll Control," *AIAA Paper 2002-1719*, 2002.
8. Cesnik, C. E. S. and Su, W., "Nonlinear Aeroelastic Modeling and Analysis of Fully Flexible Aircraft," *AIAA Paper 2005-2169*, 2005.
9. Su, W. and Cesnik, C. E. S., "Dynamic Response of Highly Flexible Flying Wing," *AIAA Paper 2006-1636*, 2006.
10. Patil, M. J. and Hodges, D. H., "Flight Dynamics of Highly Flexible Flying Wings," *Journal of Aircraft*, Vol. 43, No. 6, 2006, pp. 1790–1799.
11. Patil, M. J. and Taylor, D. J., "Gust Response of Highly Flexible Aircraft," *AIAA Paper 2006-1638*, 2006.
12. Palacios, R. and Cesnik, C. E. S., "Static Nonlinear Aeroelasticity of Flexible Slender Wings in Compressible Flow," *AIAA Paper 2005-1945*, 2005.
13. Palacios, R., Murua, J., and Cook, R., "Structural and Aerodynamic Models in Nonlinear Flight Dynamics of Very Flexible Aircraft," *AIAA Journal*, Vol. 48, No. 0, 2010, pp. 2648–2659.
14. Hesse, H. and Palacios, R., "Consistent Structural Linearisation in Flexible-Body Dynamics with Large Rigid-Body Motion," *Computers & Structures*, Vol. 110–111, No. 11, 2012, pp. 1–14.
15. Fung, Y. C., *An introduction to the theory of aeroelasticity*, John Wiley & Sons, Inc., New York, NY, 1955.